



Title	Single amino acid substitution in Plasmodium yoelii erythrocyte ligand determines its localization and controls parasite virulence
Author(s)	Otsuki, Hitoshi; Kaneko, Osamu; Thongkukiatkul, Amporn; Tachibana, Mayumi; Iriko, Hideyuki; Takeo, Satoru; Tsuboi, Takafumi; Torii, Motomi
Citation	PNAS, 106(17), pp.7167-7172; 2009
Issue Date	2009-04-28
URL	http://hdl.handle.net/10069/22077
Right	Copyright ©2009 by the National Academy of Sciences

This document is downloaded at: 2020-09-17T23:54:35Z

Classification: BIOLOGICAL SCIENCES: Microbiology

Title: Single amino acid substitution in *Plasmodium yoelii* erythrocyte ligand determines its localization and controls parasite virulence

Hitoshi Otsuki^{*}, Osamu Kaneko^{*†‡}, Amporn Thongkukiatkul^{*§}, Mayumi Tachibana^{*}, Hideyuki Iriko^{*¶}, Satoru Takeo^{||}, Takafumi Tsuboi^{||}, Motomi Torii^{*}

* Department of Molecular Parasitology, Ehime University Graduate School of Medicine, Toon, Ehime 791-0295, Japan

† Department of Protozoology, Institute of Tropical Medicine (NEKKEN) and the Global COE Program, Nagasaki University, Nagasaki, Nagasaki 852-8523, Japan

§ Department of Biology, Burapha University, Amphur Muang, Chonburi 20131, Thailand.

¶ Department of Microbiology and Pathology, Faculty of Medicine, Tottori University, Yonago, Tottori 683-8503, Japan

|| Cell-Free Science and Technology Research Center, Ehime University, Matsuyama, Ehime 790-8577, Japan

‡To whom correspondence should be addressed: Tel.: (+81)-95-819-7838; fax: (+81)-95-819-7805; E-mail: okaneko@nagasaki-u.ac.jp (O. Kaneko)

Abstract

The major virulence determinant of the rodent malaria parasite, *Plasmodium yoelii*, has remained unresolved since the discovery of the lethal line in the 1970s. As virulence in this parasite correlates with the ability to invade different types of erythrocytes, we evaluated the potential role of the parasite erythrocyte binding ligand, PyEBL. We found one amino acid substitution in a domain responsible for intracellular trafficking between the lethal and non-lethal parasite lines, and, furthermore, that the intracellular localization of PyEBL was distinct between these lines. Genetic modification showed that this substitution was responsible not only for PyEBL localization, but also the erythrocyte-type invasion preference of the parasite, and subsequently its virulence in mice. This previously unrecognized mechanism for altering an invasion phenotype indicates that subtle alterations of a malaria parasite ligand can dramatically affect host-pathogen interactions and malaria virulence.

Key words: erythrocyte, invasion, ligand, malaria, *Plasmodium yoelii*

Author contributions: H.O., O.K. and M.To. designed research; H.O., A.T., M.Ta., H.I., and S.T. performed research; T.T. contributed new reagents/analytic tools; H.O., O.K., and M.To. analyzed data; and H.O. and O.K. wrote the paper. The authors declare no conflict of interest.

Introduction

The rodent malaria parasite *Plasmodium yoelii yoelii* has been widely studied in order to understand the interactions between the malaria parasite and the host-cell (1). The non-lethal 17X line mainly infects young erythrocytes (reticulocytes) whereas the lethal 17XL and YM lines infect a wide range of erythrocytes. These lines have previously been studied in order to identify the genetic determinants of virulence (2, 3). These differences in erythrocyte invasion preference suggest the possible involvement of a parasite ligand that recognizes erythrocyte surface receptors, however, the actual molecular basis of the observed invasion preference differences remains unclear.

Erythrocyte invasion by the malaria merozoite is a multistep process, initiated by reversible binding to the erythrocyte surface, followed by the establishment of a tight junction between the apical end of the merozoite and erythrocyte surface and the subsequent movement of the merozoite into the nascent parasitophorous vacuole. Each step involves specific interactions between parasite ligands and erythrocyte receptors. Among the ligands of malaria parasites, the best characterized is a type I integral transmembrane protein encoded by the *eb1* (*erythrocyte-binding-like*) gene family. Upon release from the micronemes, EBL proteins recognize erythrocyte receptors and initiate the formation of the tight junction.

The importance of EBL in malaria virulence is exemplified in the human malaria parasite *Plasmodium vivax* which uses an EBL ortholog, PvDBP, to recognize the Duffy antigen on the erythrocyte surface. As the parasite is apparently unable to utilize an alternative invasion pathway, individuals in whom the Duffy antigen is not expressed on the erythrocyte surface are completely resistant to *P. vivax* (4, 5). Due to this dramatic association between the disruption of a host-pathogen interaction and protection against a malaria parasite, PvDBP and the *Plasmodium falciparum* EBL ortholog, EBA-175, have been targeted for vaccine development (6).

EBL proteins possess two Cys-rich regions conserved among EBL orthologs. The N-terminal Cys-rich region named the DBL (Duffy-Binding-Like) domain or Region 2 (7) recognizes a specific erythrocyte surface receptor. The C-terminal Cys-rich region named the C-cys domain or Region 6 is located adjacent to the transmembrane domain and the number and location of Cys residues are well conserved among known *Plasmodium* species. Region 6 exhibits structural similarity to the KIX-binding domain of the coactivator CREB-binding protein (8) and has been proposed to be a protein trafficking signal for transportation to the micronemes (9). Here we report a single non-synonymous nucleotide substitution in the *pyebl* gene between lethal and non-lethal lines of *P. yoelii* and show the effect of this substitution on the intracellular localization of EBL, erythrocyte-type preference and

consequently virulence of *P. yoelii*.

Results

In order to investigate differences in EBL between lethal and non-lethal *P. yoelii* lines, we compared sequences from a variety of malaria parasite species and *P. yoelii* lines 17X, 17XL, and YM. We found one non-synonymous nucleotide substitution in Region 6 between non-lethal 17X and lethal 17XL lines in the entire open reading frame (Fig. 1). The non-lethal 17X line possesses 8 conserved Cys residues that form 4 disulfide bridges (8), whereas the lethal 17XL line possesses an Arg instead of Cys at the second Cys position. This substitution was also found in another lethal line “YM” (2), which originated independently from the 17X line during serial passage (3). All *Plasmodium* EBL orthologs for which protein expression was validated possess 8 conserved Cys residues in this region, further indicating that these Cys residues play an important role (Fig. S1). Thus the observed substitution from Cys to Arg is likely to abolish the native conformation of Region 6.

EBL localizes in the dense granules in *P. yoelii* line 17XL. We raised specific polyclonal and monoclonal antibodies against PyEBL and performed Western blot analysis. The PyEBL protein was detected as a 110-kDa band in both the 17X and 17XL lines (Fig. 2A). The intracellular localization of PyEBL in both the 17X and 17XL lines was compared by indirect immunofluorescent assay (IFA) using specific antibodies against PyEBL (Fig. S2). In the 17X line, PyEBL localized to the apical end of each merozoite in both the segmented schizont-stage parasite and individual merozoites where it colocalized with AMA1, a known microneme protein, under immunofluorescent microscopy (Fig. 2B). However, in the 17XL line PyEBL did not colocalize with AMA1 at the apical end of merozoites and showed a more diffused but granular distribution in comparison with parasites of the 17X line (Fig. 2B). Diffused localization of PyEBL was also observed in parasites of the YM line (Fig. S3). Immunoelectron microscopy revealed that PyEBL localized in micronemes in the 17X line as reported for *P. falciparum* and *Plasmodium knowlesi* (9, 10). In the 17XL line, however, PyEBL localized not in the microneme, but in another microorganelle - the dense granules (12) (Fig. 2C, Fig. S4).

Since there appears to be only one copy of PyEBL in the genomes of both lines (Fig. S5) and significant differences were not observed in the level of transcription and protein expression between the 17X and 17XL lines (Fig. 2A, Fig. S6), the location of EBL appears to be the most significant difference between them.

Genetic replacement of Arg and Cys in Region 6 alters EBL localization. To evaluate if the Arg substitution at the second Cys position is responsible for the altered trafficking of PyEBL, we exchanged Cys and Arg in the 17X and 17XL lines by genetic modification (17X-CtoR and 17XL-RtoC). The parasites were also transfected with control constructs which do not alter the Region 6 amino acid sequence (17X-CtoC and 17XL-RtoR) (Fig. 3A). Each of the transgenic parasites were evaluated for the correct integration of the constructs to the *pyebl* gene locus by specific PCR analysis followed by sequencing of the

PCR-amplified products (not shown) and Southern blot analysis (Fig. 3B).

In the 17X line, replacement of Cys with Arg (17X-CtoR) altered the PyEBL localization from an apical pattern to a non-apical diffused pattern and PyEBL did not colocalize with AMA1. Furthermore, the replacement of Arg with Cys in the 17XL line (17XL-RtoC) altered the PyEBL localization from a non-apical diffused pattern to an apical pattern. Control parasites did not display altered PyEBL localization (Fig. 4). These results confirm that the observed substitution from Cys to Arg is responsible for the altered localization of PyEBL from micronemes to dense granules in the 17XL line.

EBL localization alters erythrocyte-type preference and course of infection. In order to determine if altered localization of PyEBL affects erythrocyte-type invasion preference, infected erythrocytes were examined by microscopy and a selectivity index (SI) was obtained by calculating multiple parasite infection of single erythrocytes for each parasite line on day 3 post-infection in mice (13). We found that 17XL-RtoC predominantly invaded reticulocytes in the same way as the non-lethal 17X line. The SI of the 17XL line (2.38) was increased in 17XL-RtoC (~35; $P < 0.001$). On the other hand, 17X-CtoR was able to invade a variety of ages of erythrocytes including mature erythrocytes, comparable to the lethal 17XL line, with the SI of the 17X line (16.78) reduced in 17X-CtoR (~4; $P < 0.001$; Table. 1). These results demonstrate that the localization of PyEBL is responsible for the erythrocyte-type preference of the parasite.

As erythrocyte-type preference frequently correlates with virulence in malaria parasites, we further analyzed the transgenic *P. yoelii* parasites for differences in the course of infection and survival of parasite-infected mice. Mice infected with the 17XL-RtoC line developed significantly lower parasitemias compared with the parental 17XL and control 17XL-RtoR lines (Fig. 5A) with 100% survival (Fig. 5C), whereas all mice infected with 17XL and 17XL-RtoR lines died by day 7 (Fig. 5C). The pattern observed for the 17XL-RtoC line was identical to that observed for the non-lethal 17X line. Thus, trafficking of PyEBL to the micronemes causes the virulence of the 17XL line to be reduced to the same level as the non-lethal 17X line, suggesting that PyEBL is a critical virulence determinant in the 17XL line. The parasitemia of mice infected with 17X-CtoR increased significantly compared to those infected with parental 17X and control 17X-CtoC lines during the acute phase of infection on days 4 to 5 ($P < 0.001$). However, the parasitemia did not reach the level observed for the lethal 17XL line, and reduced to the same level observed for the 17X and 17X-CtoC lines by day 9 (Fig. 5B). No parasites were detectable by microscopy at day 17 (not shown). This suggests that the 17X-CtoR line is able to invade a greater repertoire of erythrocyte types than 17X, but is unable to invade as many types as the 17XL line. This reduced capacity to invade multiple erythrocyte types compared to the 17XL line results in a non-lethal infection, in which all mice survive (Fig. 5C). Thus, displacement of the EBL from microneme was not sufficient to make this line fully lethal, suggesting the existence of other determinant(s).

Discussion

The results of this study indicate that replacement of Cys to Arg at the second Cys position of PyEBL Region 6 is the major determinant of the difference between lethal and non-lethal lines of *P. y. yoelii* parasites. This substitution alters the intracellular organelle localization of PyEBL from the micronemes to the dense granules, and alters the erythrocyte-type invasion preference, course of infection and parasite virulence in the host.

The crystal structure of Region 6 of *P. falciparum* EBA-175 indicates that the second Cys residue forms a disulfide bridge with the fourth Cys residue in this region. Arg substitution of the second Cys residue in the *P. yoelii* 17XL line abolishes this disulfide bridge, and thus likely destroys the Region 6 structure which is critical for the trafficking of the protein to the micronemes. It is possible that incorrectly folded Region 6 would not allow the protein to be properly recognized by an (as yet uncharacterized) partner molecule responsible for the trafficking of the EBL protein to the micronemes (9). The mechanism involved in the trafficking of the mutated protein to the dense granules remains unresolved.

Using genetic modification, we have demonstrated that when PyEBL is trafficked to the microneme in the 17XL line genetic background, the erythrocyte-type invasion preference and the course of infection are comparable with those of the non-lethal 17X line. This indicates that the substitution of Cys to Arg is a major determinant of the lethal phenotype of the 17XL line. However, when PyEBL was not trafficked to the microneme in parasites with the 17X line genetic background, the course of infection was intermediate between the two parental lines, suggesting that although PyEBL is a critical determinant, other factor(s) are also involved in the lethal phenotype of the 17XL line. In *P. falciparum*, the expression of EBL appears to be co-operationally regulated with another *Plasmodium* ligand encoded by the *rbl* (*reticulocyte-binding-like*) multigene family that is composed of 6 members in *P. falciparum* and at least 14 members in *P. yoelii* (14 - 16), thus the *P. yoelii* *rbl* protein, Py235, is a potential candidate for such factor(s). Consistent with this hypothesis is the finding that when Py235 expression was suppressed, the course of infection of the lethal *P. yoelii* YM line was altered from a lethal pattern to an intermediate pattern similar to that observed in the 17X-CtoR line shown in this study (17). Based on these observations, we propose that PyEBL may preferentially recognize reticulocytes and that the removal of PyEBL from the micronemes may result in free space within this organelle that may subsequently be filled with other ligand(s), possibly Py235, which consequently enables the parasite to invade a variety of erythrocyte types. As different Py235 proteins may have different receptor-specificities, parasite invasion preference and the subsequent course of infection may vary, depending on the Py235 member that fills the free space in the micronemes created by the absence of PyEBL. Such a switching mechanism for an erythrocyte invasion pathway has been previously proposed for *P. falciparum* (18).

A Linkage Group Selection analysis conducted by Pattaradilokrat *et al* [submitted together with this manuscript] identified a chromosomal region which included the *eb1* gene locus as a major determinant in the multiplication rate differences between the lethal *P. y.*

yoelii YM line and a non-lethal 33X line, supporting the role of the EBL protein in controlling virulence phenotypes. Consistent with our findings that another genetic factor may be involved, they also identified a further genomic region on *P. yoelii* chromosome 5 or 6 that showed weak association with multiplication rate.

As PyEBL localized in the dense granules is potentially non-functional, we attempted to disrupt the *pyebl* gene locus in both the 17X and 17XL lines (Fig. S7). However, repeated attempts failed to achieve this, despite the successful genomic integration of the control plasmid. This indicates PyEBL is essential for parasite survival even when it is not trafficked to the microneme. Two possible explanations for this may be; an undetectable amount of PyEBL may still localize in the micronemes and remain functional, or PyEBL is functional during erythrocyte invasion (or for another unknown critical role during the life cycle) even when localized in the dense granules. Although a subgroup of the dense granules, known as exonemes, were recently reported to secrete their contents immediately prior to schizont rupture (19), we found that PyEBL was not detected on the surface of released individual merozoites of 17XL parasites (Fig. S8). Thus, the identity of the PyEBL-containing dense granules and the timing of PyEBL secretion from them, if at all, in the 17XL line remain undetermined.

In summary, we have found that a single nucleotide substitution altered the intracellular localization of the malaria parasite ligand PyEBL, which in turn altered erythrocyte invasion preference, course of infection, and parasite virulence. The virulence-mediating mechanism described in this report furthers our understanding of parasite-host interactions, and has important implications for malaria vaccine design especially those based on PvDBP for *P. vivax* malaria.

Materials and Methods

Rodent malaria parasites. *Plasmodium yoelii* 17X, 17XL, and YM lines were maintained in BALB/c mice (Charles River Japan Inc., Japan). *P. yoelii* YM line was a kind gift from David Walliker, Edinburgh University, UK.

DNA and RNA isolation. Parasite genomic DNA (gDNA) was isolated from parasite-infected mouse blood using DNAzol BD reagent (Invitrogen, Carlsbad, CA). Parasite-infected blood was passed through one CF11 cellulose column to remove leukocytes and a schizont-enriched fraction was collected by differential centrifugation on a 50% Percoll™ solution (GE Healthcare, Buckinghamshire, UK). Total RNA was isolated from the schizont-enriched fraction using RNeasy Mini Kit (QIAGEN, Germany). Complementary DNA (cDNA) was synthesized using Omniscript reverse transcriptase (QIAGEN) with random hexamer after DNase treatment.

PCR amplification and sequencing of *eb1* genes. *eb1* genes were PCR-amplified from gDNA using KOD Plus DNA polymerase (TOYOBO, Japan) with specific primers for each *eb1* gene designed using the *P. yoelii* genome database (The Institute for Genomic Research website) and the *P. chabaudi* and *P. berghei* genome project' databases (The Sanger Centre website). *eb1* sequences were determined by direct sequencing using an ABI PRISM® 310 genetic analyzer (Applied Biosystems, Foster City,

CA) from PCR-amplified products. Sequences were aligned in CLUSTALW implemented in MacVector (ver. 9.0; Accelrys, Inc., San Diego, CA).

Southern blot analysis. Five micrograms of *P. yoelii* gDNA were digested with *EcoRI*, *EcoRV*, *Clal*, *BanI* and *NspI*, and *BanI* and *HpaI* with appropriate buffer overnight. Digested gDNA was subjected to electrophoresis on 0.8% agarose gels, followed by alkaline transfer onto a Hybond-N+ PVDF membrane (GE Healthcare). Probes were firstly PCR-amplified with 5'-TAAATCTAAATGGGATACAT-3' and 5'-AGTTGGATTGATAGTTACAGATTC-3' primers for the *pyeb1* region (Pr), cloned into pGEM-T Easy® plasmid (Promega, Madison, WI), digested from the plasmid, and then hybridized onto membranes. Probes were labeled with the AlkPhos Direct kit (GE Healthcare) and a chemi-luminescent signal developed with CDP-*star* reagent (GE Healthcare) was recorded on RX-U film (FUJI-FILM, Japan).

Recombinant proteins. Expression plasmids were constructed based on the pEU-E01-G(TEV)-N2 vector (20) by inserting PCR products amplified from *P. yoelii* 17X gDNA using KOD Plus DNA polymerase with following primers: 5'-gagaCTCGAGGTTAATTTATTA AAAAGA ACATAT GAATCTTTCC-3' and 5'-tctcGGATCCCTATGAATAGCTCTCTTTTGGAAA C-3' for *PyEBL* regions 1 to 6 (R1-6; amino acid positions 28 – 787), 5'-gagaCTCGAGGTTAATTTATTA AAAAGA ACATAT GAATCTTTCC-3' and 5'-tctcGGATCCCTACAAATTATTATTAATAGGAGT ATTACTGGG-3' for regions 1 to 2 (R1-2; 28 – 436), 5'-gagaCTCGAGGAAAAAATGGAAATGTAAATTA CAAAG-3' and 5'-tctcGGATCCCTACAAATTATTATTAATAGGAGT ATTACTGGG-3' for region 2 (R2; 113 – 436), 5'-gagaCTCGAGTCTTCTGTAAACCCAGTAATAC-3' and 5'-tctcGGATCCCTATACATTTTCGTTGGCTAGC-3' for regions 3 to 5 (R3-5; 423 – 716), and 5'-GAGAGAGACTCGAGGACCCTAAACATGTATGT GTTGATAC-3' and 5'-GAGAGAGAGGATCCTCATCCATAAAGCTGGA AGAACTACAG-3' for the 19-kDa region of the merozoite surface protein 1, *PyMSP1* (*PyMSP1*-19; 1658 – 1757). The stop codon is shown in bold letters and *XhoI* and *BamHI* restriction sites are underlined. Glutathione S-transferase (GST)-fused *PyEBL* or *PyMSP1*-19 recombinant proteins were expressed using the wheat germ cell free protein synthesis system (Protomist DT, CellFree Sciences, Matsuyama, Japan). Recombinant proteins were captured by a glutathione column, washed, and eluted with glutathione elution buffer. Protein synthesis was confirmed by SDS-PAGE and Coomassie Brilliant Blue protein staining. Recombinant *PyEBL* R1-6 and R3-5 and *PyMSP1*-19 were used to produce antibodies and *PyEBL* R1-2, and R2 were used for Western blot analysis.

Antibodies. To produce mouse anti-*PyEBL* and anti-*PyMSP1* sera, female BALB/c mice were intraperitoneally immunized 5 times with recombinant *PyEBL* R1-6 or 3 times with recombinant *PyMSP1*-19

emulsified with Freund's adjuvant, and sacrificed for serum collection. To produce rabbit anti-*PyEBL* R3-5 serum, a female Japanese white rabbit was subcutaneously immunized 3 times with recombinant *PyEBL* R3-5 emulsified with Freund's adjuvant. To produce mouse anti-*PyEBL* monoclonal antibodies, the spleen was removed from a mouse immunized with recombinant *PyEBL* R1-6 and spleen cells were fused with a mouse myeloma cell line derived from a BALB/c mouse by conventional polyethylene glycol method. Supernatants of cultured hybridoma colonies were tested with recombinant *PyEBL* R1-6 by enzyme-linked immunosorbent assay and on *P. yoelii* 17 X blood smears by indirect immunofluorescent assay. Positive hybridoma colonies were selected and cloned by two rounds of limiting dilution. The epitope region of each monoclonal antibody was tested by Western blot with a panel of recombinant *PyEBL* proteins. Anti-AMA1 rabbit serum was a gift from Carole Long, National Institutes of Health, USA.

Immunofluorescence microscopy. *P. yoelii*-infected mouse erythrocytes were smeared onto glass slides, air dried and stored at -80°C without fixation. Slides were thawed, acetone-fixed, preincubated with PBS containing 5% non-fat milk at 37°C for 30 min, incubated with mouse anti-*PyEBL* and rabbit anti-AMA1 sera at room temperature for one hour, and then incubated with fluorescein isothiocyanate (FITC)-conjugated goat anti-(mouse IgG and IgM) antibody (Biosource Int., Camarillo, CA) and Alexa-546 conjugated goat anti-rabbit IgG antibody (Molecular Probes, Eugene, OR) at 37°C for 30 min. Parasite nuclei were stained with 4',6-diamidino-2-phenylindole (DAPI). Differential interference contrast (DIC) and fluorescent images were obtained using a fluorescence microscope (BX50; Olympus, Japan) with a CCD digital camera (DC500; Leica, Germany), and processed using Adobe Photoshop CS (ver. 8.0; Adobe Systems Inc., San Jose, CA).

Immunoelectron microscopy. *P. yoelii*-infected mouse blood was fixed in 1% paraformaldehyde-0.1% glutaraldehyde in HEPES-buffered saline, and embedded in LR white resin (Polysciences, Inc., Warrington, PA). Sections were blocked for 30 min in PBS-milk-Tween 20, incubated overnight at 4°C in PBS-milk-Tween 20 containing mouse anti-*PyEBL* R1-6 serum, and then incubated for 1 hour in PBS-milk-Tween 20 containing goat anti-mouse IgG conjugated with gold particles (10 nm diameter; Jansen, Piscataway, NJ). Sections were stained with 2% uranyl acetate in 50% methanol and examined by electron microscopy (JEM-1230; JEOL, Japan).

Genetic modification of the *pyeb1* gene locus. Two basic plasmids, pPbDT3U-B12 and pHDEF1-mh-R12, were constructed. A DNA fragment encoding cyan fluorescent protein (CFP) was PCR-amplified from pECFP-C1 plasmid (Stratagene) using KOD Plus DNA polymerase with primers 5'-agcGCTAGCGTGAGCAAGGGCGAG-3' (*NheI* site is underlined) and 5'-gacGTCGACGGATCCTCTAGACTTGACAGCTC GTCC-3' (*Sall* and *XbaI* sites are underlined and *BamHI* site is shown in bold), and ligated into the pGEM-T Easy plasmid. The insert was then digested with *NheI* and *Sall*, purified, and ligated into pRGDT-B12 (21) using the *NheI*

and *SalI* sites, yielding pRCDT-B12. pRCDT-B12 was digested with *ClaI* and *XbaI* and filled with a oligonucleotide linker comprising cgatCTCGAGCCCCGGGt and ctagaCCCCGGGCTCGAGat to generate *XhoI* (underlined) and *SmaI* (bold) sites to yield pPbDT3U-B12. pHDEF1-mh (22) was digested with *SmaI* and *ApaI* to remove the 3' untranslated region of histidine rich protein 2, the *ApaI* cohesive end was blunted and a Gateway gene conversion cassette C1 (Invitrogen) was inserted. The *XhoI* site was destroyed by *XhoI*-digestion, filled-in using KOD Plus DNA polymerase, and self-ligated to yield pHDEF1-mh-R12.

To modify the *pyebl* gene locus, a DNA fragment encoding *PyEBL* region 6 to the stop codon was PCR-amplified from gDNA of the *P. yoelii* 17XL line with primers

5'-gCCATGGGAACATAGAGACATTAATAAAAAGC-3' and

5'-gCTCGAGATAAAAATCTACAGGTATATATTC-3' (*NcoI* and *XhoI* sites are underlined) and cloned into pGEM-T Easy[®] plasmids. The insert was ligated into the *NcoI* and *XhoI* sites of pPbDT3U-B12 to yield pR6Cyt-B12. DNA fragments encoding *PyEBL* region 3 to the stop codon were PCR-amplified from cDNA of *P. yoelii* 17X and 17XL lines with primers

5'-atCTTCTGTAAACCCAGTAATAC-3' and

5'-ccAGATCTTTAATAAAAATCTACAGGTATATATTC-3' (*BglIII* site is underlined). PCR products were then ligated into the *SmaI* site of pR6Cyt-B12, yielding pR6Cyt+R3Cyt(X)-B12 and pR6Cyt+R3Cyt(XL)-B12, respectively.

pR6Cyt+R3Cyt(X)-B12 and pR6Cyt+R3Cyt(XL)-B12 were subjected to a BP recombination reaction with the donor vector pDONRTM221 (Invitrogen) to produce the corresponding entry plasmids pENT.R6Cyt+R3Cyt(X) and pENT.R6Cyt+R3Cyt(XL). These entry plasmids were subjected to a LR recombination reaction (Invitrogen) according to the manufacturer's instructions with pHDEF-1-mh-R12 to yield replacement constructs pYEBL-R6Cyt+R3Cyt(X) and pYEBL-R6Cyt+R3Cyt(XL), respectively.

P. yoelii schizont-enriched fraction was collected by differential centrifugation on 50% HistoDenz in PBS and 20 µg of *XhoI*-digested transfection constructs were electroporated to 5×10^7 of enriched schizonts using the NucleofectorTM device (Amaxa GmbH, Germany) with Human T cell solution under program U-33 (23). Transfected parasites were intravenously injected into 8-week-old BALB/c female mice, which were treated by intraperitoneal injection with 1 mg/kg of pyrimethamine daily. Before inoculation of 17X line parasites, mice were treated with phenylhydrazine to increase the reticulocyte population in the blood. Drug resistant parasites were cloned by limiting dilution. Integration of the transfection constructs was confirmed by PCR-amplification with a unique set of primers for the modified *pyebl* gene locus followed by sequencing, and Southern blot analysis.

Course of infection. To assess the course of infection of transgenic and wild type parasite lines, 1×10^6 parasitized erythrocytes were injected intravenously into 8-week-old female BALB/c mice. Thin blood smears were made daily, stained with Giemsa's solution, and parasitemias were recorded. Mouse survival was evaluated by the

Kaplan-Meier method. Parasitemias of each group were compared by one-way ANOVA test and Tukey's post test implemented in Prism4.0 (GraphPad Software, San Diego, CA).

Selectivity index. To compare erythrocyte preference between transgenic and wild type *P. yoelii* parasite lines, a selectivity index was calculated as follows; multiple-infected erythrocytes divided by the expected number of multiple-infected erythrocytes, which was calculated from the number of infected erythrocytes and parasitemia (13). When the preferred erythrocyte type is limited, the observed number of multiple-infected erythrocytes increases. More than 200 parasitized erythrocytes were examined on Giemsa-stained thin blood smears collected on day 3 post-inoculation. The selectivity index of each group was compared by one-way ANOVA test and Tukey's post test implemented in Prism4.0.

ACKNOWLEDGMENTS. This work was supported in part by Grants-in-Aids for Scientific Research 19790308 (to HO) and 19590428 (to OK) from the Ministry of Education, Culture, Sports, Science and Technology, Japan, and by JSPS-NUS Joint Research Program 07039011-000161 (to OK). We thank D. Walliker for *P. yoelii* 33X, 33XPr3 and YM lines; C. Long for anti-AMA1 rabbit serum; H. A. del Portillo for pHDEF1-mh; Y. Tanaka, K. Kameda and K. Oka, INCS, Ehime University for their expertise; N. Kangwanransan for anti-*PyMSP1-19* serum; and R. Culleton for critical reading. Preliminary sequence data for *P. berghei*, *P. chabaudi* and *P. vinckei* were obtained from The Institute for Genomic Research (<http://www.tigr.org>). Nucleotide sequence data reported in this paper are available in the GenBankTM/EMBL/DBJ databases under the accession numbers: AB430781 – AB430789. Animal experiments were carried out in compliance with the Guide for Animal Experimentation at Ehime University School of Medicine.

References

1. Landau I, Gautret P, in *Malaria: Parasite Biology, Pathogenesis, and Protection*, I. W. Sherman, Ed. (American Society for Microbiology, Washington, DC, 1998), pp. 401-417.
2. Yoeli M, Hargreaves B, Carter R, Walliker D (1975) Sudden increase in virulence in a strain of *Plasmodium berghei yoelii*. *Ann Trop Med Parasitol* 69:173-178.
3. Playfair JH, De Souza JB, Cottrell BJ. (1977) Protection of mice against malaria by a killed vaccine: differences in effectiveness against *P. yoelii* and *P. berghei*. *Immunology* 33:507-515.
4. Miller LH, Mason SJ, Clyde DF, McGinniss MH (1976) The resistance factor to *Plasmodium vivax* in blacks. The Duffy-blood-group genotype, FyFy. *N Engl J Med* 295, 302-304.
5. Wertheimer SP, Barnwell JW (1989) *Plasmodium vivax* interaction with the human Duffy blood group glycoprotein: identification of a parasite receptor-like protein. *Exp Parasitol* 69:340-350.
6. Greenwood BM, Fidock DA, Kyle DE, Kappe SH, Alonso PL, Collins FH, Duffy PE (2008) Malaria: progress, perils, and prospects for eradication. *J Clin Invest* 118:1266-1276.

7. Adams JH, Sim BK, Dolan SA, Fang X, Kaslow DC, Miller LH (1992) A family of erythrocyte binding proteins of malaria parasites. *Proc Natl Acad Sci U S A* 89:7085-7089.
8. Withers-Martinez C, Haire LF, Hackett F, Walker PA, Howell SA, Smerdon SJ, Dodson GG, Blackman MJ (2008) Malarial EBA-175 region VI crystallographic structure reveals a KIX-like binding interface. *J Mol Biol* 375:773-781.
9. Treeck M, Struck NS, Haase S, Langer C, Herrmann S, Healer J, Cowman AF, Gilberger TW (2006) A conserved region in the EBL proteins is implicated in microneme targeting of the malaria parasite *Plasmodium falciparum*. *J Biol Chem* 281:31995-32003.
10. Sim BK, Toyoshima T, Haynes JD, Aikawa M (1992) Localization of the 175-kilodalton erythrocyte binding antigen in micronemes of *Plasmodium falciparum* merozoites. *Mol Biochem Parasitol* 51:157-159.
11. Adams JH, Hudson DE, Torii M, Ward GE, Wellems TE, Aikawa M, Miller LH (1990) The Duffy receptor family of *Plasmodium knowlesi* is located within the micronemes of invasive malaria merozoites. *Cell* 63:141-153.
12. Torii M, Adams JH, Miller LH, Aikawa M (1989) Release of merozoite dense granules during erythrocyte invasion by *Plasmodium knowlesi*. *Infect Immun* 57:3230-3233.
13. Simpson JA, Silamut K, Chotivanich K, Pukrittayakamee S, White NJ (1999) Red cell selectivity in malaria: a study of multiple-infected erythrocytes. *Trans R Soc Trop Med Hyg* 93:165-168.
14. Stubbs J, Simpson KM, Triglia T, Plouffe D, Tonkin CJ, Duraisingh MT, Maier AG, Winzeler EA, Cowman AF (2005) Molecular mechanism for switching of *P. falciparum* invasion pathways into human erythrocytes. *Science* 309:1384-1387.
15. Iyer J, Grüner AC, Rénia L, Snounou G, Preiser PR (2007) Invasion of host cells by malaria parasites: a tale of two protein families. *Mol Microbiol* 65:231-249.
16. Carlton JM, Angiuoli SV, Suh BB, Kooij TW, Perteau M, Silva JC, Ermolaeva MD, Allen JE, Selengut JD, Koo HL, et al. (2002) Genome sequence and comparative analysis of the model rodent malaria parasite *Plasmodium yoelii yoelii*. *Nature* 419:512-519.
17. Iyer JK, Amaladoss A, Ganesan S, Preiser PR (2007) Variable expression of the 235 kDa rhoptry protein of *Plasmodium yoelii* mediate host cell adaptation and immune evasion. *Mol Microbiol* 65:333-346.
18. Duraisingh MT, Maier AG, Triglia T, Cowman AF (2003) Erythrocyte-binding antigen 175 mediates invasion in *Plasmodium falciparum* utilizing sialic acid-dependent and -independent pathways. *Proc Natl Acad Sci U S A* 100:4796-4801
19. Yeoh S, O'Donnell RA, Koussis K, Dluzewski AR, Ansell KH, Osborne SA, Hackett F, Withers-Martinez C, Mitchell GH, Bannister LH, et al. (2007) Subcellular discharge of a serine protease mediates release of invasive malaria parasites from host erythrocytes. *Cell* 131:1072-1083.
20. Tsuboi T, Takeo S, Iriko H, Jin L, Tsuchimochi M, Matsuda S, Han ET, Otsuki H, Kaneko O, Sattabongkot J, et al. (2008) Wheat germ cell-free system-based production of malaria proteins for discovery of novel vaccine candidates. *Infect Immun* 76:1702-1708.
21. Ghoneim A, Kaneko O, Tsuboi T, Torii M (2007) The *Plasmodium falciparum* RhopH2 promoter and first 24 amino acids are sufficient to target proteins to the rhoptries. *Parasitol Int* 56:31-43.
22. Fernandez-Becerra C, de Azevedo MF, Yamamoto MM, del Portillo HA (2003) *Plasmodium falciparum*: new vector with bi-directional promoter activity to stably express transgenes. *Exp Parasitol* 103:88-91.
23. Janse CJ, Franke-Fayard B, Mair GR, Ramesar J, Thiel C, Engelmann S, Matuschewski K, van Gemert GJ, Sauerwein RW, Waters AP (2006) High efficiency transfection of *Plasmodium berghei* facilitates novel selection procedures. *Mol Biochem Parasitol* 145:60-70.

Figure legends

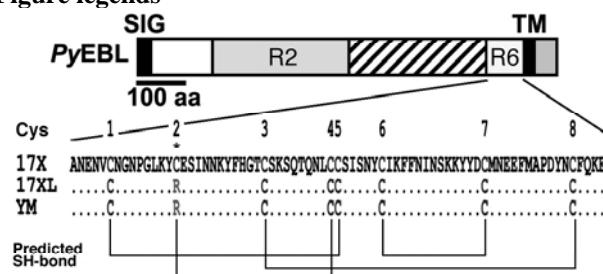


Figure 1. Schematic structure of *P. yoelii* EBL (PyEBL). SIG, TM, R2 and R6 indicate the putative endoplasmic reticulum transporting signal, the transmembrane region, Region 2 and Region 6. Amino acid alignment of PyEBL from 17X, 17XL and YM lines are shown below. Eight conserved Cys residues that form disulfide bridges (Predicted SH-bond) and the substitution from Cys to Arg (*) are indicated.

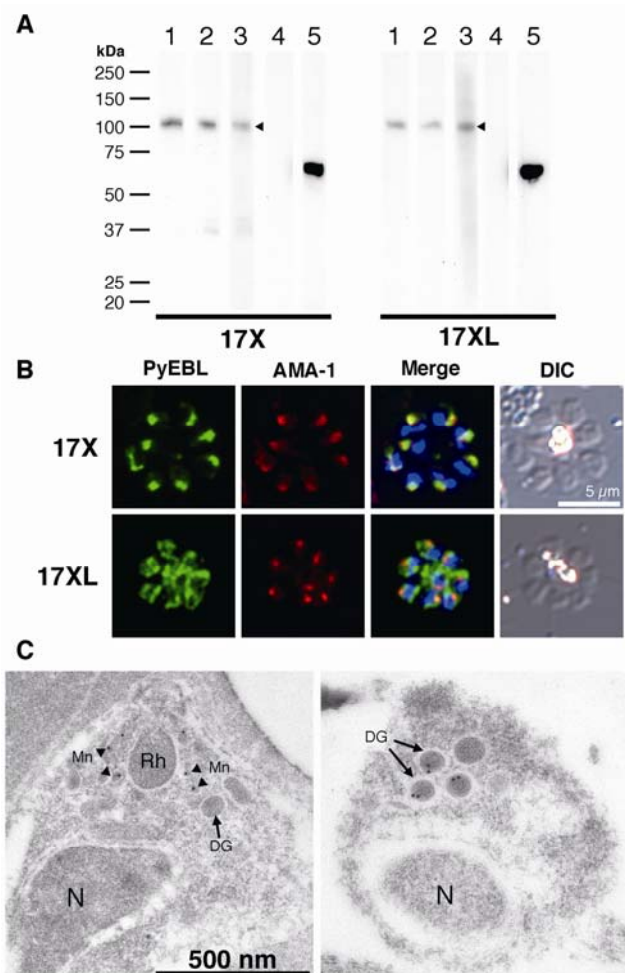


Figure 2. Western blot analysis and PyEBL localization in *P. yoelii* schizont by immunostaining. (A) Western blot analysis with monoclonal antibodies (mAb) 5B10 (lane 1), mAb 1G10 (lanes 2) and mouse serum (lane 3) specific for PyEBL against purified *P. yoelii* schizont extracts. A 110-kDa band was detected in both 17X and 17XL lines with no significant difference in the protein expression level (arrowhead). This band was not detected by normal mouse serum (lane 4). Anti-AMA1 serum detected 66-kDa band in the similar level (lane 5). (B) *P. yoelii* schizonts were incubated with mAb 5B10 (α -EBL), rabbit anti-AMA1 serum (α -AMA1), and DAPI (blue) for nuclear staining. Schizonts labeled with anti-PyEBL (5B10) were stained with FITC secondary antibody (green). Anti-AMA1 were stained with Alexa-546 secondary antibody (red). Differential interference contrast (DIC) images are shown in the right-hand column. 17X line shows apical PyEBL signal co-localized with AMA1, but region 6 substituted 17XL line shows diffused staining that does not co-localize with AMA1. (C) Immunoelectron microscopy was carried out for resin-embedded *P. yoelii* 17X and 17XL lines with anti-PyEBL mouse serum and secondary antibody conjugated with gold particles. PyEBL was detected in the micronemes (arrowheads) of the 17X line, but in the 17XL line, it was located in the dense granules (arrows). N, Mn, DG and Rh indicate nucleus, microneme, dense granule and rhoptry.

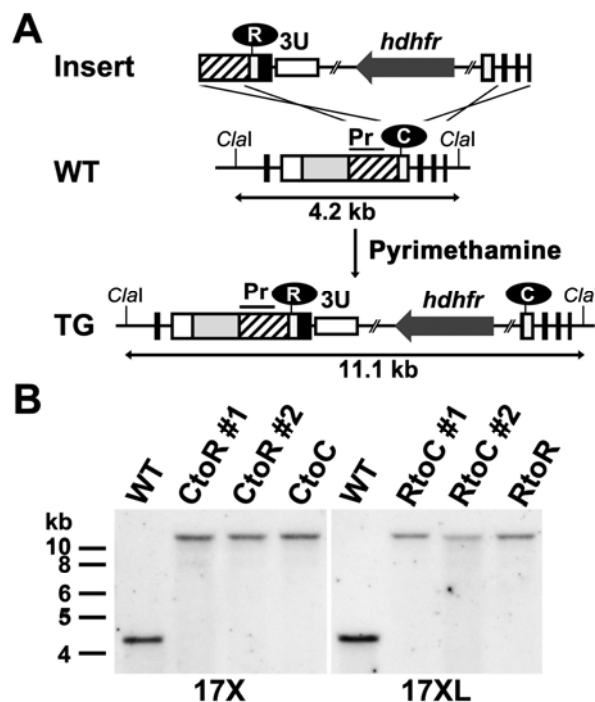


Figure 3. Amino acid replacement of PyEBL region 6 second cysteine location by targeted recombination. (A) Schematic representation of the wild-type (WT) and modified (TG) *pyebl* gene loci. The replacement cassette (Insert) was inserted into the *pyebl* gene locus by double crossover recombination. In this schematic, the second Cys in Region 6 was replaced with Arg in the 17X line to generate 17X-CtoR. Other transgenic lines were generated in a similar fashion. *Clal* restriction sites and the expected size of the DNA fragment following *Clal* digestion are shown. "Pr" indicates a probe region used in Southern blot analysis. (B) Southern blot analysis of the *pyebl* gene locus in WT and transgenic parasite lines derived from *P. yoelii* 17X and 17XL. The absence of the 4.2-kb WT band and the presence of an 11.1-kb band indicate that the PyEBL locus was modified in all transgenic clones.

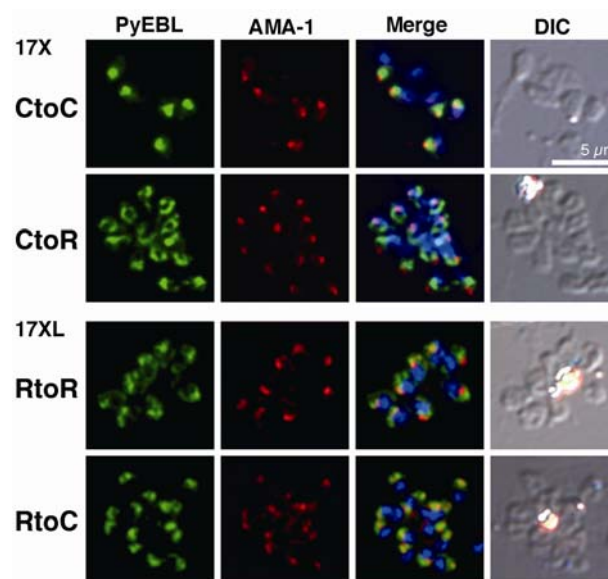


Figure 4. Replacement of Cys to Arg in Region 6 altered subcellular localization of PyEBL. Schizonts of transgenic parasite lines were incubated with mAb 5B10 (α -EBL), rabbit anti-AMA1 serum (α -AMA1), and DAPI (blue) for nuclear staining. DIC images are shown in the right-hand column. In 17X background, control (C to C)

shows apical *PyEBL* signal co-localized with AMA1, but replaced (C to R) shows 17XL pattern. Inversely, 17XL background control (R to R) shows diffused non-apical pattern, but replaced to cysteine (R to C) shows apical and co-localized with AMA1.

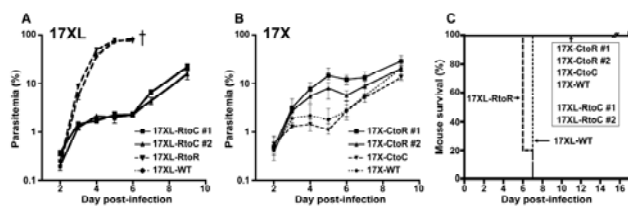


Figure 5. Effect of the alteration of *pyebl* gene loci on the course of infection and parasite virulence in mice. Mice were intravenously inoculated with 1×10^6 parasitized

erythrocytes from wild type or transgenic parasite lines. (A) Parasitemia of 17XL-RtoC was dramatically reduced to the same level as that of the non-lethal 17X line. (B) Parasitemia of 17X-CtoR was significantly higher than parental 17X and control 17X-CtoC on days 4 and 5 ($P < 0.001$), the acute phase of infection, however the pattern observed is intermediate between the lethal 17XL and non-lethal 17X lines. Parasitemias are plotted using the geometric mean and standard deviation of log-transformed data from groups of 5 mice. (C) All mice infected with 17XL-RtoC survived whereas all mice infected with parental 17XL and control 17XL-RtoR lines died by day 7. All mice infected with 17X, 17X-CtoC and 17X-CtoR survived.

Table legends

TABLE 1. Selectivity index of wild type and transgenic *Plasmodium yoelii* lines.

Parasite	n	Selectivity Index	(range)
17X-CtoR #1	5	3.87	(1.86 - 5.32)
17X-CtoR #2	5	4.25	(2.38 - 7.97)
17X-CtoC	5	23.53	(16.49 - 36.00)
17X	5	16.78	(7.60 - 24.99)
17XL-RtoC #1	5	34.35	(29.18 - 38.05)
17XL-RtoC #2	5	35.99	(29.97 - 42.72)
17XL-RtoR	5	1.31	(0.57 - 2.13)
17XL	5	2.38	(1.58 - 3.75)

Selectivity indices were calculated from parasitized Giemsa stained thin blood films collected from each infection.

Supporting Online Material

Supplementary Materials and Methods

Quantification of *pyebl* and *pyama1* transcripts. To quantify and compare *pyebl* transcription levels between 17X and 17XL, real-time PCR was carried out under the following conditions; five BALB/c mice were infected with *P. yoelii* intraperitoneally and parasites were collected on day 5 by cardiac puncture. Total RNA was isolated from each mouse independently and cDNA was generated from the schizont enriched fraction. Real-time PCR was carried out using the QuantiTect™ SYBR® Green PCR Kit (QIAGEN) with 5'-TGAATCTTTCCAATCTTTCCC-3' and 5'-CCATGTCTCTCCGTTTCAATG-3' primers for *pyebl* or with 5'-GAAAAGGTGCATGGTTCTGG-3' and 5'-GAAAAGGTGCATGGTTCTGG-3' primers for *pyama1* using the LightCycler® system (F. Hoffmann-La Roche Ltd., Basel, Switzerland). Copy number of *pyebl* and *pyama1* were determined using a standard curve generated by serially diluted plasmids containing the target insert sequence.

SDS-PAGE and Western blot analysis. Parasite-infected blood was passed through a CF11 cellulose column to remove leukocytes and a schizont-enriched fraction was collected by differential centrifugation on a 50% Percoll solution. Schizont proteins were first extracted by repeated freezing-thaw cycles in phosphate buffered saline (PBS) containing protease inhibitors [PI; 1 µg/mL of leupeptin, 1 µg/mL of pepstatin A, 100 µM 4-(2-aminoethyl) benzenesulfonyl fluoride hydrochloride] and 1 mM EDTA (ethylenediaminetetraacetic acid), followed by extraction of the insoluble pellet in 1% Triton X-100 in PBS-PI. Triton X-100 soluble proteins, containing PyEBL and PyAMA1, were incubated with 6% β-mercaptoethanol at 100°C for 3 min, and subjected to electrophoresis on a 5–20% polyacrylamide gel (ATTO, Japan). Proteins were then transferred to a Immuno-Blot PVDF membrane (Bio-Rad, Hercules, CA), immunostained with mouse serum or monoclonal antibodies followed by horseradish peroxidase-conjugated goat anti-(mouse IgG Fc) antibody (The Jackson laboratory, Bar Harbor, ME), and visualized with Immobilon™ Western Chemiluminescent HRP substrate (Millipore, Billerica, MA). Images were captured on RX-U film.

Live staining of *P. yoelii* free merozoites. Parasitized erythrocytes collected from mice were suspended in RPMI1640 medium containing 20% fetal calf serum (complete medium) and incubated at 24°C for 13 hours for schizont maturation. Schizonts were then enriched by differential centrifugation on 50% HistoDenz (Sigma, St. Louis, MO) in PBS at 2,500 rpm for 12 min. Collected parasites were passed through a 29G syringe needle 5 times, suspended in 500 µl of RPMI1640 complete medium, and then incubated at 37°C for 2 min. Parasites were washed, incubated in RPMI1640 complete medium containing rabbit anti-PyEBL R3-5 and mouse anti-PyMSP1-19 sera at room temperature for 30 min, washed again, and smeared on glass slides. Air dried smears were fixed in ice-cold acetone, and incubated with Alexa-488 conjugated goat anti-rabbit IgG antibody (Molecular Probes) and Alexa-546 conjugated goat

anti-mouse IgG antibody. Parasite nuclei were stained with DAPI. Images were captured as described above.

Knock-out strategy of the *pyebl* gene locus. To knock-out the *pyebl* gene locus, a DNA fragment from the 5' side of *pyebl* was PCR-amplified from gDNA of the *P. yoelii* 17XL line with primers 5'-ACCAAATGCATAGAGTTTTA-3' and 5'-AAATTGATTCTTCTACTTGGTATG-3'. PCR products were then ligated into *Sma*I site of pR6Cyt-B12, yielding pR6Cyt+5U-B12, which was processed in a similar manner as described above to yield knock-out construct pYEBL-KO.

Supplementary Figure legends

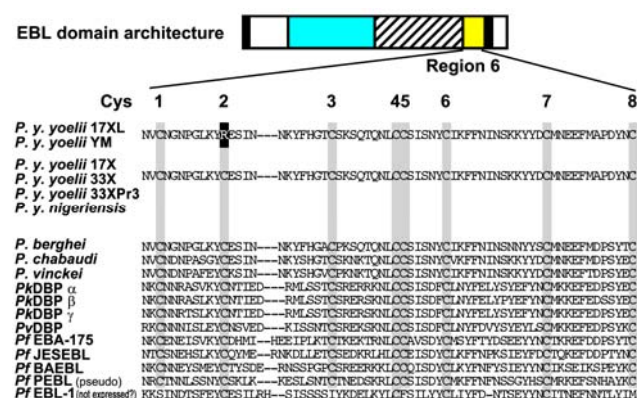


Figure S1. Alignment of the deduced amino acid sequence of *Plasmodium* EBL region 6. Cys residues are highlighted and numbered. *P.y.*, *Plasmodium yoelii*; *PkDBP* α , β , and γ (M90466, M90694, and M90695, respectively), *Plasmodium knowlesi* Duffy Binding Proteins; *PvDBP* (DQ156512), *Plasmodium vivax* DBP; *PfEBA-175* (M93397), *PfJESEBL* (AB080796), *PfBAEBL* (AF332918), *PfPEBL* (DQ100425), and *PfEBL1* (AF131999), *Plasmodium falciparum* EBLs. Nucleotide sequences for *P. y. yoelii* EBL 17XL line (AB430781), YM line (AB430783), 17X line (AB430782), 33X line (AB430784), and 33XPr3 line (AB430785), *P. y. nigeriensis* EBL (AB430786), *P. berghei* EBL (ANKA line, AB430787), *P. chabaudi* EBL (AB430788), and *P. vinckei* EBL (AB430789) are deposited in DDBJ. The number and location of Cys residues in region 6 are conserved among 17 EBL proteins except *P. yoelii* 17XL and YM lines, and *PfEBL-1*. The transcription of *PfEBL-1* has been shown to below, the transcription pattern throughout the asexual life cycle was distinct from other members, and protein expression has not been observed to date. *P. yoelii* 33X, 33XPr3 and YM lines are kind gifts from D. Walliker. Preliminary sequence data for *P. berghei*, *P. chabaudi* and *P. vinckei* were obtained from The Institute for Genomic Research (<http://www.tigr.org>). Nucleotide sequence data reported in this paper are available in the GenBank™/EMBL/DDBJ databases under the accession numbers: AB430781 – AB430789.

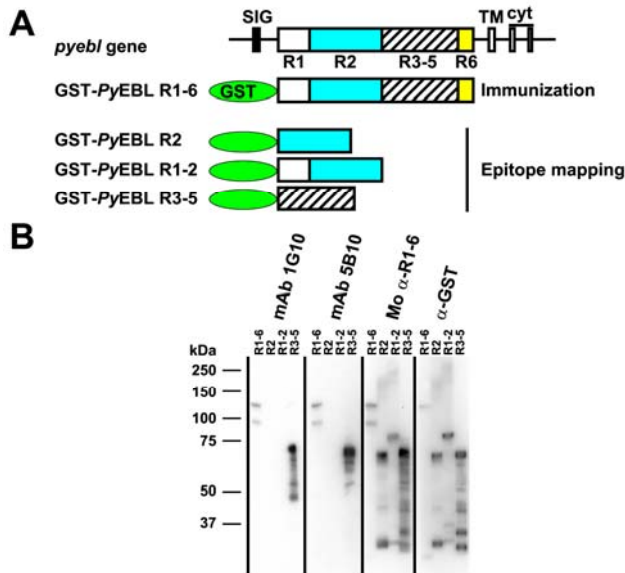


Figure S2. Recombinant EBL proteins and anti-PyEBL antibodies. (A) Schematic representation of a panel of glutathione S-transferase (GST)-fused PyEBL recombinant proteins used for immunization and/or epitope mapping of antibodies. SIG, predicted signal peptide sequence; TM, transmembrane region; cyt, cytoplasmic region; R1, R2, R3-5, and R6 indicate PyEBL regions 1 to 6. (B) Epitope mapping of antibodies. Western blot analysis showed that monoclonal antibodies (mAb) 1G10 and 5B10 reacted with GST-PyEBLR1-6 and GST-PyEBLR3-5, indicating that the epitope was located in PyEBL region R-5. Mouse anti-PyEBLR1-6 serum (Mo α -R1-6) reacted with all recombinant PyEBL proteins.

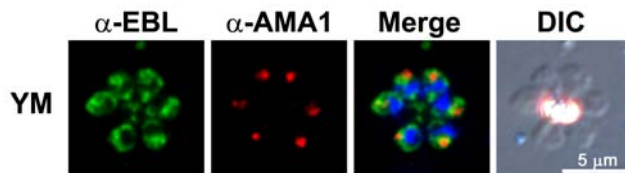


Figure S3. Subcellular localization of EBL in *Plasmodium yoelii* YM line. *P. yoelii* YM line schizonts were incubated with mAb 5B10 (α -EBL; FITC, green), rabbit anti-AMA1 serum (α -AMA1; Alexa-546, red), and DAPI (blue) for nuclear staining. Differential interference contrast (DIC) images are shown in the right-hand panel. EBL did not co-localize with AMA1 in the YM line, similar to the observation in 17XL line.

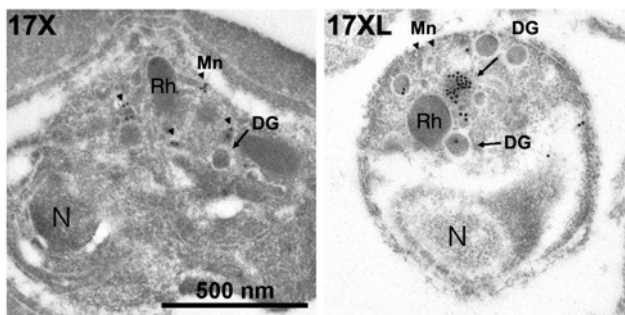


Figure S4. Further immunoelectron microscopy images. PyEBL was detected in the micronemes (arrowheads) in the 17X line, however, it was detected in the dense granules (arrows) in 17XL line. N, Mn, DG and Rh indicate nucleus, micronemes, dense granules and rhoptries.

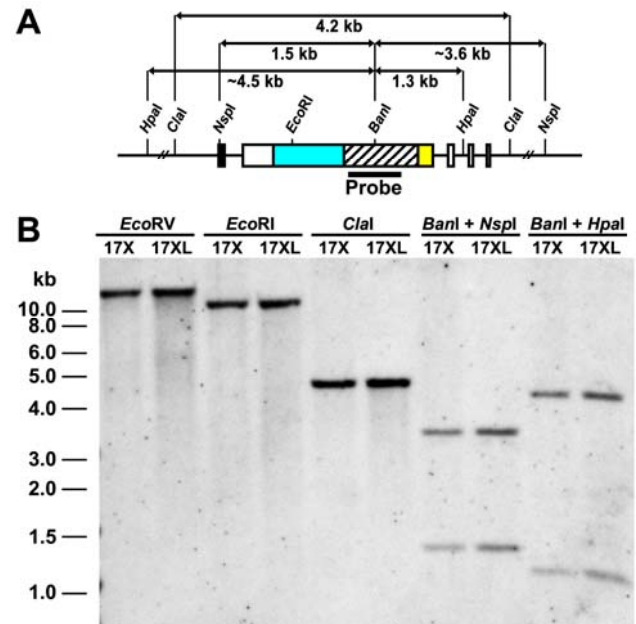


Figure S5. *pyebl* is a single copy gene. (A) Schematic of the *pyebl* gene locus (not to scale). Restriction sites and the expected size of the DNA fragment by enzyme digestion are shown. “Probe” indicates the probe region used in Southern blot analysis. (B) Southern blot analysis of the *pyebl* gene locus in 17X and 17XL lines. Hybridization of *pyebl* probe detected only a single band from *EcoRI*- or *EcoRV*-digested DNA and only two bands from *BlnI/HpaI*- or *BlnI/NspI*-digested DNA. If the *P. yoelii* genome possesses more than a single copy of *pyebl*, additional bands are likely to be observed. Taken together with the fact that only a single copy of the *pyebl* gene can be found in the *P. yoelii* (17X line) genome database (5-fold coverage), this result strongly suggests that *pyebl* is a single copy gene in both the 17X and 17XL lines.

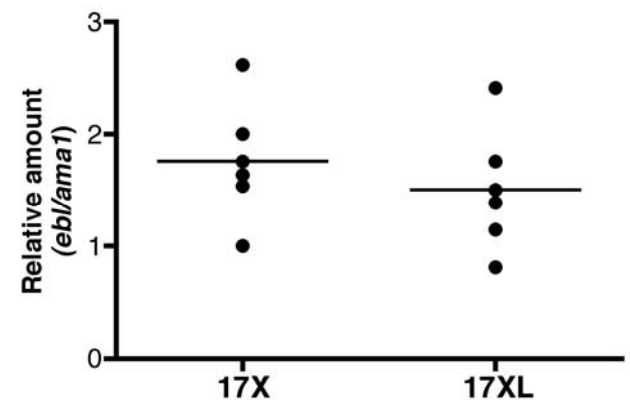


Figure S6. Quantitative comparison of PyEBL transcription. No significant difference between 17X and 17XL in the relative transcript number of *pyebl* against *ama1* quantified by real-time RT-PCR ($n = 5$). The bars indicate median values.

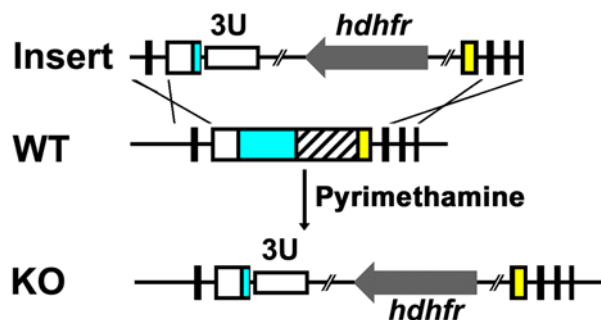


Figure S7. Knock-out strategy of the *pyebl* gene locus. Schematic of the wild-type (WT) and knock-out (KO) *pyebl* gene loci. The knock-out cassette (Insert) would be inserted into the *pyebl* gene locus by double crossover recombination and disrupts gene function. A total of 4 attempts to disrupt the *pyebl* gene locus were performed in 17X and 17XL lines (twice for each) without success. As a control, replacement plasmids, pYEBL-R6Cyt+R3Cyt(X) and pYEBL-R6Cyt+R3Cyt(XL), were simultaneously transfected and genomic integration of these plasmids was always obtained.

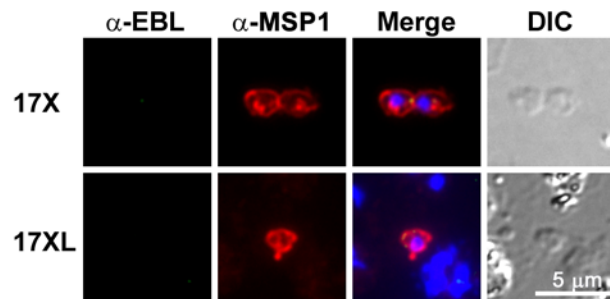


Figure S8. PyEBL was not expressed on the released merozoite surface. Live merozoites of *P. yoelii* 17X and 17XL lines were incubated with rabbit anti-PyEBL R3-5 serum (α -EBL) and mouse anti-PyMSP1-19 serum (α -MSP1), followed by secondary antibodies conjugated with fluorescent Alexa dyes and DAPI for nuclear staining. Differential interference contrast (DIC) images are shown in the right-hand column. MSP1 was detected on the merozoite surface, but EBL was not. Anti-PyMSP1-19 serum was produced by N. Kangwanrangsang, Ehime University.